Differential Localization of Vesicular Acetylcholine and Monoamine Transporters in PC12 Cells but Not CHO Cells

Yongjian Liu and Robert H. Edwards

Department of Neurology and Department of Physiology, Programs in Neuroscience and Cell Biology, University of California at San Francisco School of Medicine, San Francisco, California 94143

Abstract. Previous studies have indicated that neuroendocrine cells store monoamines and acetylcholine (ACh) in different secretory vesicles, suggesting that the transport proteins responsible for packaging these neurotransmitters sort to distinct vesicular compartments. Molecular cloning has recently demonstrated that the vesicular transporters for monoamines and ACh show strong sequence similarity, and studies of the vesicular monoamine transporters (VMATs) indicate preferential localization to large dense core vesicles (LDCVs) rather than synaptic-like microvesicles (SLMVs) in rat pheochromocytoma PC12 cells. We now report the localization of the closely related vesicular ACh transporter (VAChT). In PC12 cells, VAChT differs from the VMATs by immunofluorescence and fractionates almost exclusively to SLMVs and endosomes by equilibrium sedimentation. Immunoisolation further demonstrates colocalization with synaptophysin on SLMVs as well as other compartments. However, small amounts of VAChT also occur on LDCVs. Thus, VAChT differs in localization from the VMATs, which sort predominantly to LDCVs. In addition, we demonstrate ACh transport activity in stable PC12 transformants overexpressing VAChT. Since previous work has suggested that VAChT expression confers little if any transport activity in non-neural cells, we also determined its localization in transfected CHO fibroblasts. In CHO cells, VAChT localizes to the same endosomal compartment as the VMATs by immunofluorescence, density gradient fractionation, and immunoisolation with an antibody to the transferrin receptor. We have also detected ACh transport activity in the transfected CHO cells, indicating that localization to SLMVs is not required for function. In summary, VAChT differs in localization from the VMATs in PC12 cells but not CHO cells.

Regulated release by exocytosis involves specialized secretory vesicles that undergo fusion with the plasma membrane after the appropriate stimulation (7, 51, 53). In neuroendocrine cells, the vesicles that undergo regulated exocytosis belong to two distinct classes, synaptic vesicles (SVs)[1] and large dense core vesicles (LDCVs; 29, 37). SVs in neurons or synaptic-like microvesicles (SLMVs) in endocrine cells are small, clear vesicles that contain classical neurotransmitters such as acetylcholine (ACh), γ-aminobutyric acid (GABA), and glutamate. They cluster over the presynaptic nerve terminal and mediate the extremely rapid, precise release required for information processing. In contrast, LDCVs (or in endocrine cells, secretory granules) are larger vesicles with an electrodense core that contain neural peptides (or in the case of endocrine cells, hormones). LDCVs also differ in location from SVs, occurring in the cell body and dendrites as well as the nerve terminal. Further, different stimuli induce the exocytosis of LDCVs and SVs, and the release of LDCVs occurs over a longer time frame, consistent with the action of peptides as neuromodulators (37). The mechanism by which signaling molecules enter these secretory vesicles also differs between SVs and LDCVs. Most proteins enter the secretory compartment by co-translational translocation into the lumen of the endoplasmic reticulum (59). Thus, neural peptides already occur within the secretory compartment before they undergo sorting into LDCVs (the regulated secretory pathway). In contrast, classical transmitters are synthesized in the cytoplasm or appear there after reuptake from the extracellular space, requiring specific transport from the cytoplasm into secretory vesicles.

Previous work has identified four distinct vesicular transport activities for classical neurotransmitters (17, 50). These include one transport activity for monoamines, an-

Address all correspondence to R.H. Edwards, Department of Neurology and Department of Physiology, UCSF School of Medicine, San Francisco, CA 94143-0435. Tel. and Fax: (415) 502-5687. E-mail: edwards@itsa.ucsf.edu

1. *Abbreviations used in this paper*: ACh, acetylcholine; ChAT, choline acetyltransferase; LDCVs, large dense core vesicles; SLMVs, synaptic-like microvesicles; SV, synaptic vesicle; TfR, transferrin receptor; VAChT, vesicular ACh transporter; VMAT, vesicular monoamine transporters.

other for ACh, a third for GABA and glycine, and a fourth for glutamate. In contrast to the plasma membrane transporters that terminate transmitter action by removing them from the synaptic cleft and use the Na^+ gradient across the plasma membrane, the vesicular transporters use the H^+ electrochemical gradient across the vesicle membrane generated by a vacuolar H^+-ATPase. In particular, vesicular amine transport involves the exchange of two lumenal protons for one cytoplasmic monoamine (26), and ACh transport also uses primarily the chemical component of the electrochemical gradient (2) whereas vesicular GABA and glutamate transport depend more heavily on the electrical component (24, 30, 38).

Previous studies have indicated that neuroendocrine cells store monoamines and ACh in distinct vesicular compartments, suggesting that the transporters responsible for packaging these transmitters localize to distinct secretory vesicles. Monoamines are stored in the chromaffin granules (LDCVs) of adrenal medullary cells and SVs of central neuronal populations (55). ACh, on the other hand, has been reported to occur only in SVs (45). Interestingly, rat pheochromocytoma PC12 cells store both monoamines and ACh (22, 23, 39). Density gradient fractionation of PC12 cells has suggested that whereas monoamines occur in LDCVs, ACh occur almost exclusively in other vesicles such as SLMVs (3, 5). Thus, PC12 cells provide a model system to study the localization and sorting of both vesicular monoamine and ACh transporters within the same cell line.

Molecular cloning has recently demonstrated that the two vesicular monoamine transporters (VMATs) and a vesicular ACh transporter (VAChT) show close sequence similarity (16, 50). The VMATs were originally cloned by selection in the parkinsonian neurotoxin *N*-methyl–4-phenylpyridinium (MPP^+; 18, 34, 35). The VMATs protect against MPP^+ toxicity by sequestering the toxin in mitochondria and away from its primary site of action in mitochondria, implicating their activity in neural degeneration as well as signaling. Adrenal medullary and other nonneuronal cells express VMAT1, whereas central neuronal populations, sympathetic neurons, and histamine-containing cells express the closely related VMAT2 (46, 60). The sequences of the two proteins originally showed similarity only to a class of bacterial antibiotic resistance proteins, supporting a role in detoxification and defining a novel vertebrate gene family. The *Caenorhabditis elegans* mutant *unc-17* has a selective defect in cholinergic neurotransmission, and the sequence of the gene shows similarity to the VMATs, suggesting that the *unc-17* gene encodes a vesicular ACh transporter (1). Vertebrate homologues have since been identified and show strong similarity to both *unc-17* and the VMATs (4, 19, 48). Although VAChT expression occurs selectively in cholinergic neurons, apparently as a result of expression from the same genomic locus that encodes the biosynthetic enzyme choline acetyltransferase (ChAT; 4, 19), it has been difficult to demonstrate that the cDNA confers vesicular transport activity by heterologous expression in mammalian cell lines. Recently, however, stable PC12 transformants expressing VAChT have been shown to transport ACh (58).

To examine the localization of the vesicular transport proteins, we have raised antibodies to both rat VMATs and VAChT. As anticipated, adrenal chromaffin cells express VMAT1 on LDCVs, and PC12 cells show preferential expression of VMAT1 on LDCVs by both immunofluorescence and density gradient fractionation (36). Nonetheless, PC12 cells contain low but clearly detectable amounts of VMAT1 on SLMVs as well. In contrast, VAChT localizes to SVs by immunoelectron microscopy of brain sections (21). To determine whether VAChT also sorts to SLMVs in the same cells where the closely related VMAT1 appears in LDCVs, we have now examined the localization of VAChT in PC12 cells. By immunofluorescence, density gradient fractionation, and immunoisolation, VAChT localizes to SLMVs and endosomes, but small amounts also occur on LDCVs. Although VAChT and VMAT localization differ in PC12 cells, both transport proteins are found on the same endosomal vesicles in CHO cells. In addition, ACh transport activity does not appear to depend on localization to SLMVs, since membranes from transfected CHO cells as well as PC12 cells exhibit specific uptake of ACh.

Materials and Methods

Cell Culture

CHO cells were maintained in Ham's F12 medium with 5% FCS and PC12 cells in DME with 10% horse serum and 5% FCS. All cultures were incubated at 37°C in 5% CO_2 and contained penicillin and streptomycin. Stable transformants were produced by cotransfection with the selectable marker for resistance to neomycin as previously described (34, 35). Briefly, 10 μg of VAChT cDNA in the plasmid expression vector pcDNA-Amp (Invitrogen Corp., Carlsbad, CA) was coprecipitated with 1 μg RSV-neo and transfected into CHO and PC12 cells at 20% density using the standard calcium phosphate technique. 2 d after transfection, the cells were selected in 400 μg/ml G418. Approximately 2 wk after transfection, surviving colonies were picked and immunostained for VAChT expression. For immunofluorescence, PC12 cells were treated with nerve growth factor (50 ng/ml) for at least 3 d before staining. To label dense core vesicles for cell fractionation, PC12 cells were grown in standard medium containing 2.5 μCi/ml [^{3}H]norepinephrine (Dupont NEN, Boston, MA) for at least 6 h.

Antibody Production

The peptide CEDDYNYYSRS from the COOH terminus of rat VAChT predicted by the cDNA was synthesized and coupled to keyhole limpet hemocyanin (KLH) using *m*-maleimidobenzoyl *N*-hydroxysuccinimide ester (MBS) as previously described (36, 46). 1 mo after intradermal inoculation with 100 μg peptide conjugate in complete Freund's adjuvant, the rabbits were boosted with an additional subcutaneous 100-μg peptide conjugate in incomplete Freund's adjuvant and sera collected 10 d later to identify the animals producing antibody to VAChT. Subsequent boosts were performed under similar conditions and serum collected 10–12 d later. The serum was used for both immunofluorescence studies and Western analysis without further adsorption or purification.

Immunofluorescence

For immunostaining, cells were plated onto glass coverslips coated with poly-D-lysine and Matrigel (Collaborative Research, Inc., Waltham, MA) as previously described (6) and fixed with 4% paraformaldehyde in 0.1 M phosphate buffer, pH 7.2. After permeabilization and blocking in phosphate-buffered saline containing 2% bovine serum albumin, 1% fish skin gelatin, and 0.02% saponin for 1 h, the cells were incubated with primary antibody in the same buffer for 1.5 h at room temperature, washed three times for 10 min each in the same buffer, incubated an additional 1 h at room temperature with the appropriate secondary antibody diluted 1:100 in the same buffer, and washed again three times for 5 min each. To detect VAChT primary antibody, the secondary antibody was a goat anti–rabbit antibody conjugated to fluorescein (Cappel Laboratories, Malvern, PA). For the monoclonal antibodies to synaptophysin (Sigma Chemical Co., St.

Louis, MO) and chromogranin B (a generous gift of W. Huttner, University of Heidelberg, Heidelberg, Germany), we used goat anti–mouse antibodies conjugated to rhodamine (Cappel Laboratories). To determine the localization of transferrin receptors, CHO cells were pre-incubated in serum-free medium for 60 min at 37°C to deplete endogenous transferrin and then incubated with 50 μg/ml human transferrin conjugated to Texas red (Molecular Probes, Inc., Eugene, OR) for 30 min, rinsed quickly in cold medium, and fixed as above before immunostaining.

For confocal laser microscopy, immunofluorescence was performed as described above using secondary anti–rabbit antibodies conjugated to Cy3 and anti–mouse antibodies conjugated to Cy5 (Jackson ImmunoResearch Labs, West Grove, PA). The staining was then visualized with a confocal laser microscope (Bio Rad, Hercules, CA) and the images processed using the NIH Image program and Adobe Photoshop (Adobe Systems, Inc., Mountain View, CA).

Membrane Preparation and Cell Fractionation

Cell membranes were prepared as previously described (36). Briefly, the cells were harvested by scraping, pelleted, and resuspended in PBS containing 5 mM MgEGTA, 1 μg/ml leupeptin, and 0.2 mM diisopropylfluorophosphate (DFP) for homogenization at 10 μm clearance. Debris was then pelleted at 750 *g* for 5 min and the resulting postnuclear supernatant either loaded onto the appropriate gradient for fractionation or the membranes pelleted at 35,000 rpm for 45 min in a Beckman SW50.1.

For cell fractionation by equilibrium sedimentation, the postnuclear supernatant was layered onto a linear 0.6–1.6 M sucrose gradient containing 10 mM Hepes, pH 7.2, and centrifuged at 30,000 rpm for 6 h in an SW41 rotor (Beckman Instruments, Fullerton, CA) at 4°C. Fractions were collected from the top of the tube and stored at −70°C until analyzed.

For velocity sedimentation, the postnuclear supernatant was layered over a 5–25% glycerol gradient containing Hepes-buffered saline (0.15 M NaCl, 25 mM Hepes, pH 7.2) with 5 mM EGTA and centrifuged at 48,000 rpm for 1 h in an SW50.1 rotor (11). Fractions were collected as described above.

LDCV purification involved sequential fractionation through two density gradients (52). After incubating the PC12 cells with 2.5 μCi/ml [^{3}H]norepinephrine overnight to label the LDCVs, a postnuclear supernatant was prepared as described above in 137 mM NaCl, 5 mM KCl, 0.6 mM Na_2HPO_4, 25 mM Tris-HCl, pH 7.4 (TBS) containing 5 mM MgEGTA, 1 μg/ml leupeptin and 0.2 mM DFP. The postnuclear supernatant was then layered onto a 0.3–1.2 M sucrose gradient and sedimented at 25,400 rpm in an SW40 rotor (Beckman Instruments) for 30 min at 4°C. The fractions were collected and the radioactivity in an aliquot of each determined by scintillation counting. Pooled fractions containing the bulk of the radioactivity were then loaded onto a 0.6–1.6 M sucrose gradient and sedimented to equilibrium at 30,000 rpm in an SW40 for 12 h at 4°C.

N-Glycanase Digestion

PC12 or CHO cells were harvested and lysed in PBS containing 0.5% NP-40 and protease inhibitors. The nuclei were then sedimented and 100 μg protein from the supernatant digested overnight at 37°C in PBS containing 1.5% NP-40 with or without 0.3 U *N*-glycanase (Genzyme Corp., Boston, MA). The reaction was then stopped by dilution in sample buffer and the products analyzed by Western analysis.

Western Analysis

Aliquots of membrane preparations and the fractions from density gradients were diluted in 2× sample buffer and separated by electrophoresis through discontinuous 10% SDS–polyacrylamide gels before electrotransfer to nitrocellulose using a semi-dry apparatus (E&K, Saratoga, CA). The filters were then blocked in PBS containing 0.1% Tween-20 (TBS) and 5% nonfat dry milk, incubated in TBS with 1% nonfat dry milk and primary antibody at dilutions from 1:1,000 to 1:10,000 for 60 min at room temperature, washed three times in TBS, and incubated in appropriate secondary antibody conjugated to peroxidase for an additional 60 min before washing in TBS and visualization by enhanced chemiluminescence (Amersham Intl., Arlington Heights, IL).

Organelle Immunoisolation

Dynal beads (M-450) conjugated to secondary anti–mouse antibody were coated with monoclonal antibodies to either synaptophysin (Sigma Chemical Co.) or transferrin receptor (H68.4, a generous gift of I. Trowbridge, Scripps Research Institute, La Jolla, CA) by incubation overnight in Ca^{++}- and Mg^{++}-free PBS containing 2% FCS (immunoisolation buffer) followed by four washes in the same buffer. For each reaction, 20 μl of beads was mixed with 160 μl immunoisolation buffer and either 30 μl postnuclear supernatant or 60 μl from a density gradient fraction. The reaction mixture was incubated for 1 h at 4°C and washed four times with the same buffer. The immunoisolated vesicles were then extracted in sample buffer and subjected to Western analysis.

Acetylcholine Transport Assay

A postnuclear supernatant (S1) was prepared from either PC12 cells or CHO cells as described above but in 80 mM potassium tartrate, 20 mM Hepes, pH 6.8, 0.5 mM EGTA, 1 mM ascorbic acid, 2 μg/ml leupeptin, 0.2 mM DFP, and 50 μM echothiophate (Wyeth-Ayerst, Philadelphia, PA; 58; homogenization buffer). The P2 fraction was collected by sedimentation at 27,000 *g* for 35 min at 4°C. Sedimentation of the S2 at 200,000 *g* for 60 min yielded the P3 fraction, and both P2 and P3 were resuspended in homogenization buffer before assay as previously described (34, 58). Briefly, 100–200 μg protein in 50 μl was added to an equal volume of 100 mM potassium tartrate, 20 mM Hepes, pH 7.4, 1 mM ascorbic acid, and 50 μM echothiophate (transport buffer) with or without 50 μM vesamicol (RBI) and 5 μM carbonylcyanide-*m*-chlorophenylhydrazone (CCCP; Sigma Chemical Co.). Uptake was initiated by adding 100 μl transport buffer containing 0.8 mM ^{3}H-ACh (Dupont NEN), 10 mM ATP, and 10 mM $MgSO_4$. After incubation at 29°C for varying intervals, the reaction was terminated by rapid filtration through 0.2 μm Supor 200 filters (Gelman Sciences, Ann Arbor, MI), followed by three washes with cold transport buffer. The radioactivity bound to the filters was then measured by scintillation counting in 2.5 ml Cytoscint (ICN Biomedicals, Costa Mesa, CA). Uptake for 0 min at 29°C was subtracted as background.

Results

Antibody Production and Expression of VAChT in CHO and PC12 Cells

To localize VAChT in vivo as well as in cultured cells, we raised rabbit polyclonal antibodies to a peptide derived from the COOH terminus of the protein predicted by the rat cDNA. Coupling of the peptide to KLH through an NH_2-terminal cysteine using MBS has enabled production of antibodies to both VMATs (36, 46), and we have used a similar approach for VAChT. Like a bacterial fusion protein derived from the same region of VAChT (21), a COOH-terminal peptide generated antibodies of high titer that recognize several immunoreactive species in COS cells transfected with the VAChT cDNA but not in cells transfected with the vector alone or with the VMATs (data not shown).

We used the anti-peptide VAChT antibody to isolate stably transfected CHO and PC12 cells that express VAChT. After transfection and selection in the neomycin analog G418, we screened stable transformants by immunocytochemistry, using cell clones with mild to moderate VAChT expression for further study. Fig. 1 shows that untransfected CHO cells express no rat VAChT (rVAChT), as anticipated for a fibroblast cell line. A stable CHO transformant, however, expresses high levels of several immunoreactive species by Western analysis. These include an ~30-kD form that is reduced in the presence of protease inhibitors (data not shown) and thus appears to derive from the ~70-kD form by proteolysis in vitro. Wild-type PC12 cells express very low levels of endogenous rVAChT (Fig. 1 *A*). Since these levels limit the analysis, we have also isolated stable PC12 transformants overexpressing VAChT. The PC12 cell clone described here has higher, more easily detectable levels of rVAChT expression, with

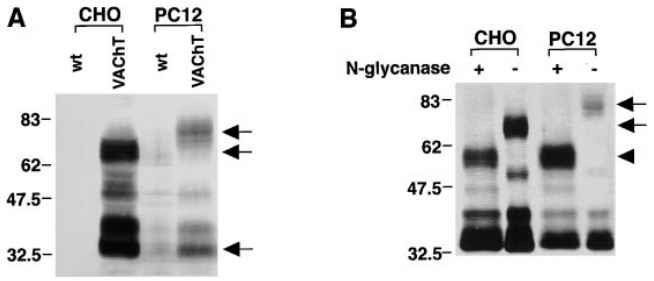

Figure 1. Western analysis of membranes from transfected CHO and PC12 cells. (*A*) An anti-peptide antibody recognizes VAChT in transfected CHO and PC12 cells. Western analysis of membranes prepared by differential centrifugation from CHO (*left*) and PC12 cells (*right*) shows that wild-type (*wt*) CHO cells express no immunoreactive VAChT, whereas a stable CHO transformant (*VAChT*) contains multiple immunoreactive forms. The two major species of ~70 and ~30 kD are indicated by the lower two arrows. Wild-type (*wt*) PC12 cells show several immunoreactive forms, most of which appear at higher levels in the stable transformant overexpressing rat VAChT. In PC12 cells, the two major species of ~80 and ~30 kD are indicated by the upper and lower arrows. Molecular masses in kD are shown to the left. (*B*) VAChT undergoes N-linked glycosylation in PC12 and CHO transformants. A postnuclear supernatant prepared from either PC12 cells (*left*) or CHO cells (*right*) was incubated overnight at 37°C in the presence (+) and absence (−) of N-glycanase. The arrows on the right indicate the undigested forms and the arrowhead the digested form of VAChT. VAChT thus undergoes N-linked glycosylation in both PC12 and CHO cells, and the extent of glycosylation differs in the two cell lines. Molecular masses (in kD) are indicated to the left.

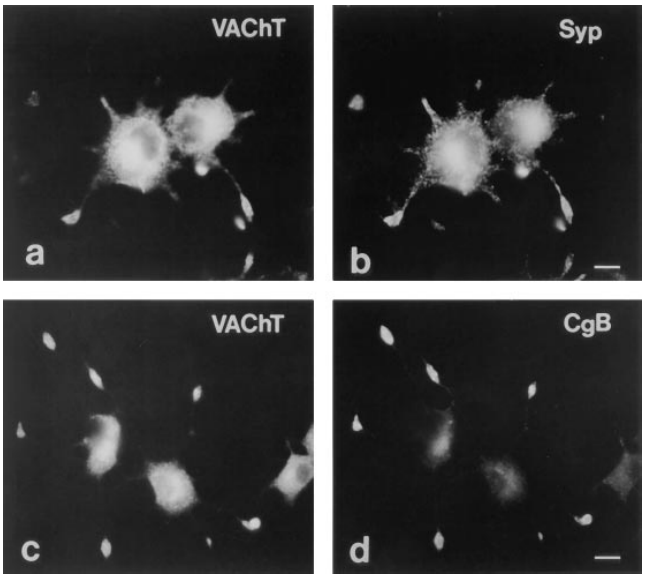

Figure 2. VAChT colocalizes with synaptophysin in wild-type PC12 cells by immunofluorescence. Wild-type PC12 cells were stained with antibodies to VAChT (*a* and *c*), synaptophysin (*b*), and chromogranin B (*d*). For double immunofluorescence of the two sets of cells (*a* and *b* and *c* and *d*), the rabbit polyclonal antibody to VAChT was detected with a secondary antibody conjugated to fluorescein and the mouse monoclonal antibodies to synaptophysin and chromogranin B were detected with a secondary antibody conjugated to rhodamine. VAChT immunoreactivity occurs at both the tips of processes and in the cell body (*a* and *c*) and colocalizes with synaptophysin at these sites (*b*). In contrast, chromogranin B occurs predominantly at the tips of processes with very little at the cell body (*d*), a pattern clearly distinct from that of VAChT (*c*). Bars, 10 μm.

an ~30-kD species similar to that observed in CHO cells but with a higher molecular species of ~80 kD as well that corresponds to the major form observed in vivo using brain extracts (21). Although the large difference in expression makes it difficult to compare the immunoreactive species in transfected and untransfected PC12 cells, they appear to differ primarily in intensity rather than size. To characterize the differences in size between transfected PC12 and CHO cells, we used N-glycanase (Fig. 1 *B*). Digestion by this enzyme reduces the immunoreactive proteins to the same size in both cell types, indicating that they differ only in the amount of N-linked carbohydrate. Indeed, we have previously observed that the glycosylation of VMATs shows similar differences between PC12 and CHO cells (36). Thus, expression of the VAChT cDNA in these two cell lines produces similar immunoreactive proteins. In addition, the anti-peptide antibody recognizes VAChT with high affinity and specificity, and the serum was used directly for subsequent studies without further purification.

Localization of VAChT in SLMVs of PC12 Cells

Previous studies have shown that SVs store ACh and exhibit ACh transport activity (45). More recently, VAChT has been localized to SVs in vivo (21, 61). However, the extent to which VAChT differs from the closely related VMATs in terms of sorting remains unclear. To compare directly the localization of VAChT and VMATs, we used PC12 cells, which store ACh and monoamines in apparently distinct vesicular compartments (3). Indeed, we have previously localized endogenous VMAT1 to LDCVs in PC12 cells (36), and VMAT2 appears to sort even more stringently to this regulated secretory pathway (Liu, Y., and R.H. Edwards, unpublished observations).

Using the anti-peptide antibodies, we first localized endogenous VAChT in untransfected PC12 cells by immunofluorescence. Fig. 2 shows that VAChT immunoreactivity appears in both the cell bodies and processes of NGF-treated cells. This coincides with the pattern observed by double immunofluorescence of the same cells for synaptophysin, a marker of SLMVs that also occurs in endosomes (8, 27), suggesting that VAChT localizes preferentially to SLMVs and endosomes. In contrast, immunofluorescence for chromogranin B, a marker of LDCVs, occurs principally at the tips of processes with only low levels of expression in cell bodies. This different pattern of expression suggests that VAChT does not localize significantly to LDCVs in PC12 cells. However, the low levels of endogenous VAChT expression preclude further analysis of its localization by biochemical methods.

To determine the localization of VAChT by quantitative methods such as density gradient fractionation, we have increased VAChT expression in PC12 cells using a variety of methods. We present the results obtained with a stable PC12 transformant, but a viral expression system has yielded similar findings (data not shown). To exclude the possibilities that overexpression of VAChT or that

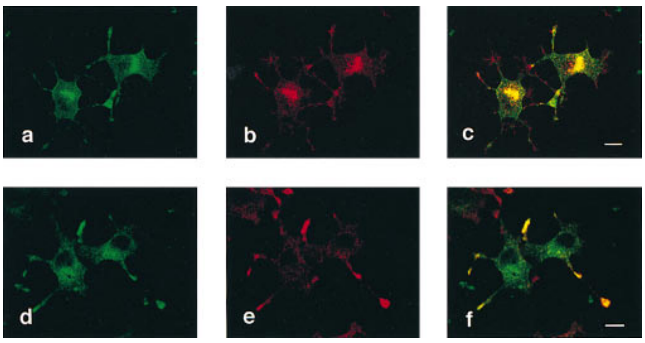

Figure 3. Colocalization of VAChT with synaptophysin in a stable PC12 cell transformant. A stable PC12 cell transformant overexpressing VAChT was immunostained for VAChT (*a* and *d*), synaptophysin (*b*), and chromogranin B (*e*). Using two sets of cells (*a–c* and *d–f*) for confocal laser microscopy, the rabbit polyclonal antibody to VAChT was detected with a secondary anti–rabbit antibody conjugated to Cy3 (*a* and *d*, *green*), and the mouse monoclonal antibody to synaptophysin was detected with a secondary anti–mouse antibody conjugated to Cy5 (*b* and *e*, *red*). The superimposed staining is shown in *c* and *f*. Similar to wild-type PC12 cells, VAChT (*a*) colocalizes with synaptophysin (*b*) at both the tips of processes and at a juxtanuclear region in the cell body (*c*, *yellow*). Despite the overexpression of VAChT in this cell line, VAChT immunoreactivity (*d*) appears quite distinct from chromogranin B (*e*), which occurs predominantly at the tips of processes and only at lower levels in the cell body (*f*, *yellow*). Bars, 10 μm.

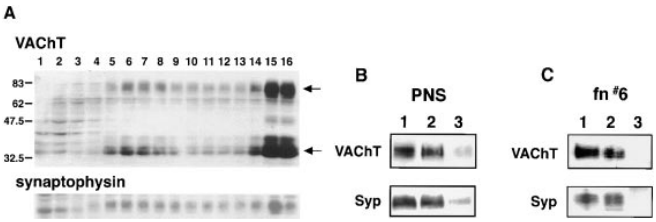

Figure 4. VAChT localizes to SLMVs by velocity sedimentation through glycerol and immunoisolation. (*A*) A stable PC12 transformant overexpressing VAChT was disrupted by homogenization and the postnuclear supernatant subjected to velocity sedimentation through a gradient of 5 to 25% glycerol. Western analysis of the fractions shows that both high and low molecular weight forms of VAChT (*arrows*) appear at a position in the middle of the gradient that coincides with synaptophysin and corresponds to SLMVs. Larger amounts of both VAChT and synaptophysin also occur at the bottom of the gradient in fractions that include endosomes. Molecular mass markers (in kD) are indicated at the left. Fractions are numbered from the top of the gradient on the left to the bottom on the right. (*B*) A postnuclear supernatant was subjected to immunoisolation using Dynal beads coated with a monoclonal antibody to synaptophysin. Western analysis using the antibody to VAChT shows substantial immunoreactivity in the starting material (lane *1*) and almost full recovery in the immunoisolated vesicles (lane *2*). Immunoisolation with uncoated Dynal beads yields minimal VAChT immunoreactivity (lane *3*). Immunostaining for synaptophysin (*Syp*) shows an identical pattern, confirming the colocalization of VAChT and synaptophysin. (*C*) Fraction 6 from the glycerol gradient was subjected to immunoisolation as described in *B*. Western analysis using the antibody to VAChT shows immunoreactivity in the starting material (lane *1*) and essentially full recovery in the immunoisolated vesicles (lane *2*). Control immunoisolation with uncoated Dynal beads yields no VAChT immunoreactivity (lane *3*). Immunostaining for synaptophysin shows an identical pattern, confirming the colocalization of VAChT and synaptophysin on the same population of SLMVs.

variation in the PC12 cell clone might produce anomalous mislocalization of the introduced protein, however, we first repeated the immunofluorescence study using the stable transformant and confocal laser microscopy. Fig. 3, *a* and *d*, shows that VAChT immunoreactivity in the PC12 clone also occurs in the cell body as well as the processes. Double staining with the SLMV marker synaptophysin (Fig. 3, *b* and *c*) shows colocalization with VAChT at a juxta-nuclear site in the cell body and partial colocalization in the processes. In contrast, the LDCV marker chromogranin B (Fig. 3, *e* and *f*) shows a complementary localization in processes rather than the cell body. Thus, heterologous expression of VAChT in this PC12 transformant does not appear to have significantly altered its localization from that of the endogenous protein, at least by immunofluorescence. Further, immunoisolation of a postnuclear supernatant with the synaptophysin antibody quantitatively precipitates all the VAChT in the starting material (Fig. 4 *B*), supporting the colocalization of VAChT and synaptophysin in this cell clone.

Using the stable PC12 transformant, we have determined the localization of VAChT by velocity gradient fractionation (Fig. 4 *A*). Velocity sedimentation through glycerol separates SLMVs from endosomes, LDCVs, and other membrane compartments. By Western analysis, synaptophysin appears both in a peak in the middle of the gradient (Fig. 4 *A*, fractions *5–8*) that represents SLMVs and at the bottom where it presumably occurs in endosomes (Fig. 4 *A*). Both high and low molecular weight forms of VAChT show a peak of similar shape in the middle of the gradient at the same position as synaptophysin, suggesting localization of VAChT in SLMVs. In addition, VAChT appears at the bottom of the gradient where, like synaptophysin, it presumably occurs in other membranes such as endosomes. To determine whether VAChT actually occurs on SLMVs, we immunoisolated vesicles from the middle of the gradient with a monoclonal antibody to synaptophysin (Fig. 4 *C*). The synaptophysin antibody precipitates essentially all of the VAChT from these fractions, whereas a control with no antibody precipitates none of the protein. Thus, VAChT occurs on the same population of SLMVs as synaptophysin.

To determine whether VAChT occurs on other membrane compartments in addition to SLMVs, we used equilibrium sedimentation through sucrose (Fig. 5). SLMVs and endosomes migrate near the top of this gradient, as shown by immunostaining for synaptophysin and TfR, respectively. In contrast, very little synaptophysin occurs toward the bottom of the gradient where LDCVs migrate, as indicated by the immunoreactivity for secretogranin II (Fig. 5, fractions *10–14*). Like synaptophysin, VAChT also appears relatively restricted to the top of the gradient. However, the peak of VAChT immunoreactivity is broad and does not coincide precisely with that for synaptophysin, suggesting expression in additional vesicular compartments. Indeed, VAChT immunoreactivity also cofractionates with

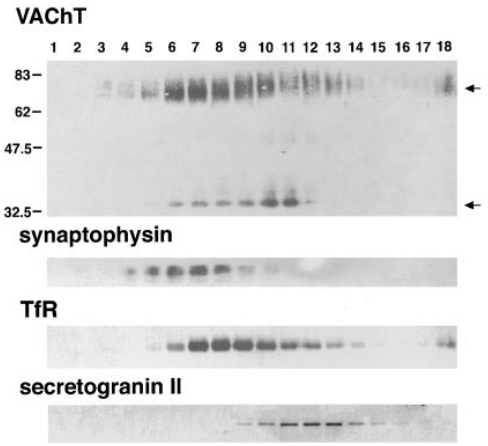

Figure 5. VAChT predominates in light membrane fractions by equilibrium sedimentation through sucrose. A postnuclear supernatant from PC12 cells overexpressing VAChT was subjected to equilibrium sedimentation through a gradient of 0.6 to 1.6 M sucrose. Western analysis shows that VAChT occurs in light membrane fractions as a very broad peak that coincides with the peak for synaptophysin, a marker of SLMVs and transferrin receptor (*TfR*), a marker of endosomes. Secretogranin II indicates fractions containing LDCVs, which migrate as a peak distinct from VAChT and synaptophysin. However, the peak of VAChT immunoreactivity overlaps with that of secretogranin II. Molecular mass markers (in kD) are indicated on the left and high and low molecular weight forms of VAChT are indicated by arrows on the right. Fractions were collected from the top of the gradient (*left*) to the bottom (*right*).

endosomal membranes expressing TfR. Nonetheless, the peak of VAChT immunoreactivity is clearly distinct from that for secretogranin II, indicating considerably lower levels of VAChT on LDCVs than on lighter vesicles such as SLMVs.

VAChT Occurs on LDCVs

Although the results indicate preferential localization of VAChT to light membranes in PC12 cells including SLMVs and endosomes, the immunofluorescence studies and density gradient fractionation cannot exclude VAChT expression on LDCVs. Localization by immunofluorescence at the tips of processes coincides with the localization of LDCVs as well as SLMVs, and the peak of VAChT expression by equilibrium sedimentation through sucrose partially overlaps with that for secretogranin II, raising the possibility that low levels of VAChT occur in LDCVs. Indeed, synaptophysin occurs at low levels on LDCVs (13, 28), suggesting that VAChT may as well. To determine whether VAChT occurs on LDCVs, we have purified LDCVs using a two-step procedure (52). After loading PC12 cells overnight with [^{3}H]norepinephrine to label the LDCVs, a postnuclear supernatant was subjected to velocity sedimentation through sucrose. This gradient separates LDCVs from a variety of membranes including endoplasmic reticulum, synaptic vesicles, and endosomes. Fractions containing LDCVs were then identified by scintillation counting and subjected to equilibrium sedimentation through sucrose. As a result of the first gradient, the second provides better separation of LDCVs from other membrane fractions, enabling detection of small amounts of proteins in LDCVs

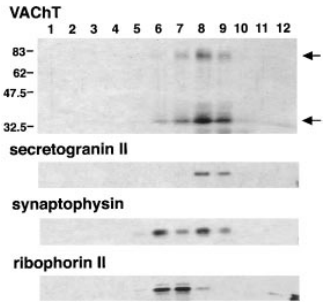

Figure 6. VAChT occurs on LDCVs by two-step density gradient fractionation. PC12 cells stably overexpressing VAChT were incubated overnight in medium containing 0.25 μCi/ml [^{3}H]norepinephrine, disrupted by homogenization, and a postnuclear supernatant subjected to two steps of density gradient fractionation. In the first step, the membranes were separated by velocity sedimentation through a gradient of 0.3 to 1.2 M sucrose. Radioactive fractions containing LDCVs in the middle of the gradient were then pooled and subjected to equilibrium sedimentation through a gradient of 0.6 to 1.6 M sucrose. Fractions from the second gradient show VAChT immunoreactivity that coincides with the LDCV marker secretogranin II as well as synaptophysin. However, some of the synaptophysin also occurs on slightly less dense vesicles that coincide with the endoplasmic reticulum marker ribophorin II. Molecular mass standards (in kD) are shown to the left and arrows indicating the two species of VAChT to the right. Fractions from the second gradient were collected from the top (*left*) to the bottom (*right*).

that occur at larger amounts in other compartments. Indeed, Fig. 6 shows a single peak of both synaptophysin and VAChT on this gradient, and in contrast to Fig. 5, which shows most of these proteins in lighter fractions, this single peak coincides with the peak of secretogranin II. Importantly, the profile of VAChT on this gradient clearly differs from that of ribophorin II, a marker for the endoplasmic reticulum. Thus, low levels of both VAChT and synaptophysin do occur specifically on LDCVs. Nonetheless, VAChT clearly differs in localization from the closely related VMATs, which occur predominantly on LDCVs.

VAChT Activity in PC12 Cells

In addition to the difference in localization of VAChT and VMATs in PC12 cells, the proteins have also appeared to differ in transport activity when expressed in a variety of cell lines. The VMATs show robust transport activity in a number of cells, but it has been more difficult to demonstrate VAChT activity. An initial report suggested uptake of ACh into intact CV-1 fibroblast cells expressing VAChT (19), but the apparent inability to demonstrate transport using either semipermeabilized cells or a membrane preparation precluded further characterization of the activity. More recently, a stable PC12 transformant expressing VAChT has been demonstrated to transport ACh with the expected functional characteristics (58). Indeed, we have identified ACh transport activity in a preparation of light membrane vesicles from transfected PC12 cells (Fig. 7 *A*). As anticipated, vesamicol inhibits this activity, and untransfected cells exhibit considerably less ACh transport.

The apparent discrepancy in function between expression of VAChT in fibroblast and neural cells raises the possibility that the localization in PC12 cells may be crucial for function. To address this possibility, we first measured [^{3}H]ACh transport in different membrane fractions from the transfected PC12 cells. Fig. 7 *B* shows little vesamicol-sensitive transport above background in a heavy

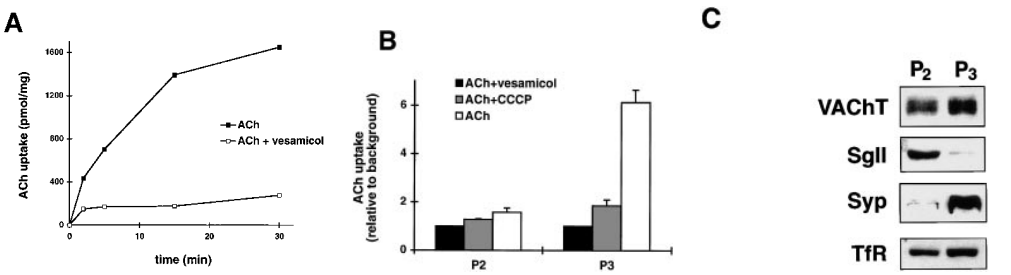

Figure 7. VAChT overexpression in PC12 cells confers vesicular ACh transport activity. (*A*) A population of light membrane vesicles (P3) from transfected PC12 cells (PC12[VAChT]; *filled squares*) demonstrates ACh transport activity substantially higher than in the same vesicles from untransfected cells (wt PC12; *filled triangles*). In addition, vesamicol inhibits the uptake by transfected cells (*open squares*) to a level lower than in untransfected cells, suggesting that endogenous PC12 cell VAChT has some transport activity. (*B*) Comparison of ACh uptake by different fractions from transfected PC12 cells. Membranes from a postnuclear supernatant collected by centrifugation at 27,000 *g* for 35 min (*P2*) show less vesamicol- and CCCP-sensitive ACh transport activity than membranes collected by centrifugation of the S2 at 200,000 *g* for 40 min (*P3*). ACh uptake is normalized to background accumulation in the presence of vesamicol for each of the membrane preparations. (*C*) Western analysis of equal amounts of protein from P2 and P3 fractions shows approximately equal amounts of VAChT and substantial amounts of transferrin receptor (*TfR*) in both fractions but considerably more of the LDCV marker secretogranin II (*SgII*) in P2 and more of the SLMV marker synaptophysin (*Syp*) in P3.

membrane fraction (Fig. 7 *B*, *P2*) prepared from the stable PC12 transformant. However, a light membrane fraction (Fig. 7 *B*, *P3*) exhibits robust transport activity that is inhibited by both vesamicol and, as expected from a known proton exchanger such as VAChT, the proton ionophore carbonyl cyanide *m*-chlorophenylhydrazone (CCCP). Western analysis demonstrates equivalent levels of VAChT protein and substantial amounts of the endosomal TfR in both fractions, but P2 clearly contains more LDCVs, as demonstrated by immunostaining for secretogranin, and P3 contains more SLMVs as shown by staining for synaptophysin (Fig. 7 *C*). Thus, VAChT activity correlates more with expression in SLMVs rather than simply the amount of the protein or its presence in endosomes, supporting the possibility that localization of VAChT to SLMVs may be crucial for function and may account for the apparent absence of detectable activity in non-neural cells. However, we also reexamined the expression of VAChT in CHO fibroblasts.

VAChT Activity in CHO Cells

To assess the localization of VAChT in non-neural cells, we have used a stable CHO transformant that also expresses VMAT1. Immunofluorescence shows particulate cytoplasmic staining for VAChT (Fig. 8). Strong immunoreactivity also occurs next to the nucleus, a pattern observed for VMAT1 as well and apparently representing the microtubule organizing center (36). To determine whether these intracellular vesicles were endosomes, we loaded the same cells with a fluorescent form of transferrin. After internalization, the fluorescence of preloaded transferrin entirely coincides with the pattern of VAChT, indicating expression of the transporter in endosomes. VMAT1 shows a similar pattern of expression in CHO cells (36), further suggesting that VAChT colocalizes with VMATs in this cell line.

We have also examined the localization of VAChT in CHO cells by sucrose density gradient fractionation. Equilibrium sedimentation of extracts from cells expressing VAChT shows a broad peak in the middle of the gradient (Fig. 9 *A*). The peak of VAChT immunoreactivity coincides with the peak of TfR as a marker for endocytic vesicles, further supporting the localization of VAChT to endosomes. Importantly, VMAT1 also expressed by these same stable transformants shows an identical pattern of localization. To confirm the localization in endosomes, we also isolated membrane vesicles from the pooled light fractions using an antibody to the TfR. The immunoisolated membranes contain a substantial proportion of total cellular VAChT, whereas control membranes isolated without antibody show little VAChT (Fig. 9 *B*). Thus, the results indicate that, in contrast to PC12 cells, VAChT colocalizes with VMATs in the endosomes of CHO fibroblasts.

Since the VMATs function in CHO cells and VAChT colocalizes with VMATs in this cell line, we assessed ACh transport activity in a postnuclear supernatant prepared from a CHO cell clone stably expressing VAChT. In contrast to membranes from untransfected cells (data not shown), vesicles from the transfected CHO cells accumulate [^{3}H]ACh in a vesamicol-sensitive manner (Fig. 10). This result indicates that VAChT does not require expression in a neural cell or in SLMVs to function.

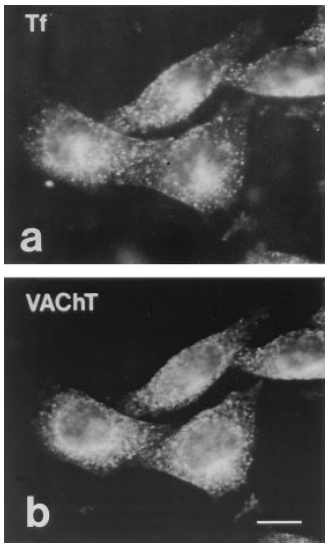

Figure 8. VAChT immunofluorescence colocalizes with transferrin receptors in transfected CHO cells. CHO cells expressing VAChT were preloaded with transferrin conjugated to Texas red. Double immunofluorescence of the same cells shows that the particulate cytoplasmic localization of internalized transferrin (*a*) coincides with the distribution of VAChT immunoreactivity (*b*). Thus, VAChT colocalizes with transferrin receptor in an endocytic compartment. Both VAChT and transferrin receptor also appear in a perinuclear compartment that occurs at the microtubule organizing center (36). Bar, 10 μm.

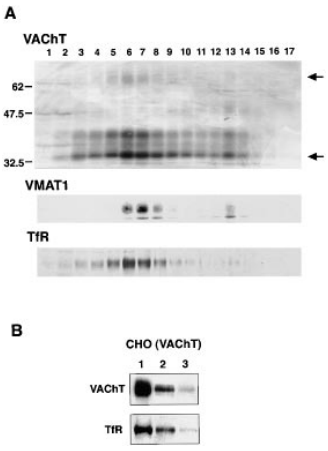

Figure 9. VAChT localizes to endosomes in CHO cells by density gradient fractionation and immunoisolation. (*A*) CHO cells expressing both VAChT and VMAT1 were homogenized and a postnuclear supernatant separated by equilibrium sedimentation through 0.6 to 1.6 M sucrose. Western analysis of the fractions shows comigration of VAChT with transferrin receptor (*TfR*), supporting the localization to endosomes indicated by immunofluorescence. Further, the peak of VAChT immunoreactivity coincides with that for VMAT1, suggesting that in contrast to PC12 cells, where they do not localize to the same membranes, VAChT and VMAT1 may colocalize in CHO cells. Molecular mass standards (in kD) are shown to the left and the two forms of VAChT indicated with arrows to the right. Fractions were collected from the top (*left*) to the bottom (*right*). (*B*) Fraction 7 from the sucrose gradient was subjected to immunoisolation using Dynal beads coated with a monoclonal antibody to the cytoplasmic domain of the transferrin receptor (H68.4). Western analysis using the antibody to VAChT shows immunoreactivity in the starting material (lane *1*) and substantial but not complete recovery in the immunoisolated vesicles (lane *2*). Immunoisolation with uncoated Dynal beads yields trace levels of VAChT immunoreactivity (lane *3*), supporting the specificity of the immunoisolation. Immunostaining for transferrin receptor (*TfR*) shows a similar pattern of incomplete recovery. Densitometry indicates that at least 20% of the total VAChT in this light membrane fraction coexists with the transferrin receptor, presumably on endosomal vesicles.

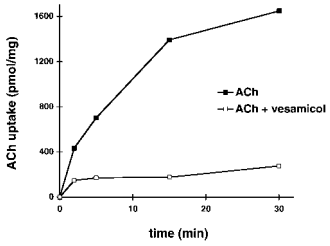

Figure 10. VAChT expression in CHO cells confers ACh transport activity. A postnuclear supernatant prepared from CHO cells stably expressing VAChT demonstrates uptake of [^{3}H]ACh (*filled squares*), which is sensitive to vesamicol (*open squares*). Membranes from untransfected cells do not exhibit vesamicol-dependent ACh transport (data not shown).

Discussion

We have characterized the localization of VAChT in PC12 cells. Immunofluorescence shows a pattern of staining similar to the SLMV marker synaptophysin and distinct from the LDCV marker secretogranin. Sucrose density gradient fractionation also indicates high levels of VAChT on light membrane vesicles consistent with location on SLMVs and endosomes. Further, velocity sedimentation through glycerol and immunoisolation of a light fraction from this gradient with an antibody to synaptophysin confirms VAChT localization to SLMVs. This distribution presumably accounts for the storage of ACh in SVs, consistent with classical observations of quantal ACh release from SVs at the neuromuscular junction, with previous studies of ACh storage and release from PC12 cells (3, 5, 23, 40, 49) and with more recent observations of VAChT localization to SVs in brain by immunoelectron microscopy (21, 61). However, the velocity gradient also demonstrates considerable amounts of VAChT in larger membranes, presumably endosomes. Synaptophysin also occurs at high levels in these endosomal fractions, apparently reflecting the inefficient biogenesis of SLMVs in PC12 cells. In addition, VAChT resides at low levels on LDCVs purified by sequential density gradient fractionation. Thus, VAChT localizes preferentially but not exclusively to SLMVs and endosomes in PC12 cells.

Although closely related in sequence, VAChT and the VMATs differ in steady-state localization in PC12 cells. In contrast to VAChT, VMAT1 localizes predominantly to LDCVs (36). Small amounts of VMAT1 occur on SLMVs in PC12 cells but at a much lower level than on heavy membrane fractions. In the brain, VMAT2 localizes to synaptic vesicles and other membranous structures (41, 42). However, VMAT2 expressed in PC12 cells occurs almost exclusively on LDCVs, with essentially none detectable on lighter membrane fractions (Liu, Y., and R.H. Edwards, unpublished observations). Thus, the predominant localization of VAChT to SLMVs and endosomes in PC12 cells differs markedly from the preferential localization of VMATs to LDCVs. The differences in steady-state localization of these closely related proteins presumably reflect differences in their membrane trafficking.

Dense core vesicles differ from synaptic vesicles in terms of biogenesis as well as in content and mode of release. LDCVs form at the TGN, where their contents appear to sort away from the constitutive secretory pathway (20, 56). In contrast, SVs form at the nerve terminal (8, 11, 47). Proteins destined for SVs enter the constitutive secretory pathway at the TGN, arrive at the cell surface, and then undergo endocytosis to form SVs (54). Thus, membrane proteins destined for SVs sort away from the regulated secretory pathway (LDCVs) at the TGN. Since VAChT occurs predominantly on SLMVs and endosomes in PC12 cells, whereas VMATs localize preferentially to LDCVs in the regulated pathway (36, 61), the TGN appears to sort these proteins to distinct secretory pathways.

The mechanisms involved in sorting to the regulated and constitutive secretory pathways remain unclear. Soluble proteins destined for the regulated pathway appear to aggregate under the appropriate conditions, indicating that they sort as a result of their general biophysical properties rather than through a specific signal (57). On the other hand, membrane proteins may sort to LDCVs through a direct interaction of their cytoplasmic domains with cytosolic proteins, a process that occurs in the retention of resident endoplasmic reticulum proteins (12), sorting to lysosomes (25), and in endocytosis (10, 43). However, very few integral membrane proteins have been identified that clearly sort to the regulated secretory pathway (14, 31). VMATs are such integral membrane proteins, and the close relationship to VAChT further suggests that a domain present in VMATs but absent from VAChT may mediate the interaction with cytosolic machinery involved in the formation of LDCVs. In this

model, trafficking to the regulated secretory pathway depends on a specific sorting event, whereas constitutive secretion occurs by default. However, it is also possible that the VAChT found in LDCVs may be removed from these vesicles as they mature.

During the process of LDCV maturation after budding from the TGN, proteins destined for lysosomes or constitutive secretion are removed from LDCVs (32, 33). Indeed, clathrin and its associated proteins associate in patches with the surface of immature secretory granules, suggesting that they may participate in selective budding and the removal of constitutively secreted proteins (15, 44, 56). VAChT may therefore undergo specific exclusion or removal from LDCVs. In this model, sorting of the VMATs to LDCVs could occur by default.

The mechanisms involved in sorting to the regulated and constitutive secretory pathways and hence the differences in trafficking between VMATs and VAChT remain poorly understood. However, the availability of two closely related integral membrane proteins that sort divergently into the two secretory pathways provides a way to address basic questions about the biogenesis of secretory vesicles. Interestingly, immunoelectron microscopy has localized VMAT2 to vesicles budding off the TGN that contain a dense core (41), whereas VAChT has a more diffuse localization in the Golgi complex (21), supporting the first model of specific sorting to the regulated secretory pathway.

Differential localization of VAChT and the VMATs in PC12 cells raises the possibility that the two types of transporter also sort differently in fibroblasts. Indeed, a recent report suggests that although fibroblasts release most secreted proteins constitutively, they retain a fraction and secrete these upon stimulation, suggesting the presence of a regulated secretory pathway (9). Since the VMATs sort to LDCVs in PC12 cells, they may also sort to this regulated pathway in fibroblasts and so acquire the capacity to function. The location of VAChT, which sorts to the constitutive pathway in PC12 cells, may thus differ from the VMATs in CHO cells as well, possibly accounting for the absence of detectable VAChT function in previous studies using non-neural cells (19, 48, 58). One report has also described uptake into whole cells (19), suggesting the presence of VAChT at the cell surface. Thus, we have also determined the localization of VAChT in CHO fibroblasts.

The results show substantial steady-state expression of VAChT in an endocytic compartment in CHO cells. Immunofluorescence, density gradient fractionation, and immunoisolation indicate extensive colocalization of VAChT with internalized TfR. Previous studies have demonstrated that other synaptic vesicle proteins localize to endosomes when expressed in fibroblast cell lines (8, 27). Presumably, the acidic nature of this compartment provides the driving force for active transport by the VMATs, and VMAT1 does localize to endosomes in CHO cells (36). In addition, we now show that VAChT colocalizes with VMAT1 expressed in the same cells. These observations in CHO cells support the impression that VAChT, like synaptophysin and other SV proteins, contains signals for endocytosis that function in fibroblasts as well as in neuroendocrine cells. The results also suggest that differences in localization cannot account for the inability to detect ACh transport, at least in CHO cells. Rather, the lack of transport may derive from the absence of a required cofactor in non-neural cells.

PC12 cells stably expressing VAChT have previously been shown to exhibit vesicular ACh transport (58). To assess the role of localization in this activity, we prepared a fraction of light membrane vesicles (P3) from PC12 cells overexpressing VAChT. These membranes exhibit accumulation of [^{3}H]ACh sensitive to the inhibitor vesamicol. Interestingly, a heavier membrane fraction (P2) shows little if any specific ACh transport activity but contains almost equivalent amounts of VAChT to P3. Western analysis further demonstrates that the P3 fraction contains much more synaptophysin but considerably less secretogranin II than the P2 fraction, suggesting that expression in SLMVs or endosomes rather than in LDCVs may be required for transport activity.

To determine whether localization to SLMVs is required for ACh transport activity, we used the stable CHO transformant expressing VAChT. A postnuclear supernatant prepared from these cells shows substantial vesamicol-sensitive accumulation of [^{3}H]ACh. Thus, VAChT can function in the endosomes of non-neural cells and does not appear to require specific synaptic vesicle proteins or other cofactors.

In summary, we demonstrate the differential localization in PC12 cells of the closely related vesicular transporters for ACh and monoamines. VAChT localizes preferentially to SLMVs and endosomes, whereas the VMATs localize predominantly to LDCVs. Since SV proteins use the constitutive, secretory pathway to reach the cell surface before recycling to SVs, the results suggest that VAChT and the VMATs sort divergently in the TGN, VAChT to the constitutive, and VMATs to the regulated secretory pathway. As integral membrane proteins, the restricted sequence differences between VAChT and the VMATs may thus provide a tool to dissect the mechanism of differential sorting in the TGN. In addition, we find that VAChT functions in non-neural as well as neural cells and so does not require expression with other SV proteins for activity.

We thank the members of the Edwards lab for thoughtful discussion and helpful suggestions. We also thank L. Clift-O'Grady and R.B. Kelly for help with the immunoisolations, M. Silver for the assistance with confocal laser microscopy, W. Huttner and D. Cutler for the secretogranin antibodies, D. Meyer for the antibody to ribophorin II, T. Weimbs and K. Mostov for monoclonal antibody H68.4 to the transferrin receptor, and W. Mobley for the generous gift of NGF.

This work was supported by grants from the National Alliance for Research on Schizophrenia and Affective Disorders (to Y. Liu) and from the Alzheimer's Program of the State of California and the National Institutes of Health (to R.H. Edwards).

Received for publication 2 June 1997 and in revised form 8 September 1997.

References

1. Alfonso, A., K. Grundahl, J.S. Duerr, H.-P. Han, and J.B. Rand. 1993. The Caenorhabditis elegans unc-17 gene: a putative vesicular acetylcholine transporter. *Science.* 261:617–619.
2. Anderson, D.C., S.C. King, and S.M. Parsons. 1982. Proton gradient linkage to active uptake of 3H-acetylcholine by Torpedo electric organ synaptic vesicles. *Biochemistry.* 21:3037–3043.
3. Bauerfeind, R., A. Regnier-Vigouroux, T. Flatmark, and W.B. Huttner. 1993. Selective storage of acetylcholine, but not catecholamines, in neuroendocrine synaptic-like microvesicles of early endosomal origin. *Neuron.* 11:105–121.

4. Bejanin, S., R. Cervini, J. Mallet, and S. Berrard. 1994. A unique gene organization for two cholinergic markers, choline acetyltransferase and a putative vesicular transporter of acetylcholine. *J. Biol. Chem.* 269:21944–21947.
5. Blumberg, D., and E.S. Schweitzer. 1992. Vesamicol binding to subcellular membranes that are distinct from catecholaminergic vesicles in PC12 cells. *J. Neurochem.* 58:801–810.
6. Bonzelius, F., G.A. Herman, M.H. Cardone, K.E. Mostov, and R.B. Kelly. 1994. The polymeric immunoglobulin receptor accumulates in specialized endosomes but not synaptic vesicles within the neurites of transfected neuroendocrine PC12 cells. *J. Cell Biol.* 127:1603–1616.
7. Calakos, N., and R.H. Scheller. 1996. Synaptic vesicle biogenesis, docking and fusion: a molecular description. *Physiol. Rev.* 76:1–29.
8. Cameron, P.L., T.C. Sudhof, R. Jahn, and P. de Camilli. 1991. Colocalization of synaptophysin with transferrin receptors: implications for synaptic vesicle biogenesis. *J. Cell Biol.* 115:151–164.
9. Chavez, R.A., S.G. Miller, and H.-P. Moore. 1996. A biosynthetic regulated secretory pathway in constitutive secretory cells. *J. Cell Biol.* 133:1177–1191.
10. Chen, W.J., J.L. Goldstein, and M.S. Brown. 1990. NPXY, a sequence often found in cytoplasmic tails, is required for coated pit-mediated internalization of the low density lipoprotein receptor. *J. Biol. Chem.* 265:3116–3123.
11. Clift-O'Grady, L., A.D. Linstedt, A.W. Lowe, E. Grote, and R.B. Kelly. 1990. Biogenesis of synaptic vesicle-like structures in a pheochromocytoma cell line PC12. *J. Cell Biol.* 110:1693–1703.
12. Cosson, P., and F. Letourneur. 1994. Coatamer interaction with di-lysine endoplasmic reticulum retention motifs. *Science.* 263:1629–1631.
13. De Camilli, P., and R. Jahn. 1990. Pathways to regulated exocytosis in neurons. *Annu. Rev. Physiol.* 52:625–645.
14. Disdier, M., J.H. Morrissey, R.D. Fugate, D.F. Bainton, and R.P. McEver. 1992. Cytoplasmic domain of P-selectin (CD62) contains the signal for sorting into the regulated secretory pathway. *Mol. Biol. Cell.* 3:309–321.
15. Dittie, A.S., N. Hajibagheri, and S.A. Tooze. 1996. The AP-1 adaptor complex binds to immature secretory granules from PC12 cells and is regulated by ADP-ribosylation factor. *J. Cell Biol.* 132:523–536.
16. Edwards, R.H. 1992. The transport of neurotransmitters into synaptic vesicles. *Curr. Opin. Neurobiol.* 2:586–594.
17. Edwards, R.H. 1993. Neural degeneration and the transport of neurotransmitters. *Annu. Neurol.* 34:638–645.
18. Erickson, J.D., L.E. Eiden, and B.J. Hoffman. 1992. Expression cloning of a reserpine-sensitive vesicular monoamine transporter. *Proc. Natl. Acad. Sci. USA.* 89:10993–10997.
19. Erickson, J.D., H. Varoqui, M.D. Schafer, W. Modi, M.F. Diebler, E. Weihe, J. Rand, L.E. Eiden, T.I. Bonner, and T.B. Usdin. 1994. Functional identification of a vesicular acetylcholine transporter and its expression from a "cholinergic" gene locus. *J. Biol. Chem.* 269:21929–21932.
20. Farquhar, M.G., J.J. Reid, and L.W. Daniell. 1978. Intracellular transport and packaging of prolactin: a quantitative electron microscope autoradiographic study of mamotrophs dissociated from rat pituitaries. *Endocrinology.* 102:296–311.
21. Gilmor, M.L., N.R. Nash, A. Roghani, R.H. Edwards, H. Yi, S.M. Hersch, and A.I. Levey. 1996. Expression of the putative vesicular acetylcholine transporter in rat brain and localization in cholinergic synaptic vesicles. *J. Neurosci.* 16:2179–2190.
22. Greene, L.A., and A.S. Tischler. 1976. Establishment of a noradrenergic clonal line of rat adrenal pheochromocytoma cells which respond to nerve growth factor. *Proc. Natl. Acad. Sci. USA.* 73:2424–2428.
23. Greene, L.A., and G. Rein. 1977. Synthesis, storage and release of acetylcholine by a noradrenergic pheochromocytoma cell line. *Nature.* 268: 349–351.
24. Hell, J.W., P.R. Maycox, and R. Jahn. 1990. Energy dependence and functional reconstitution of the γ-aminobutyric acid carrier from synaptic vesicles. *J. Biol. Chem.* 265:2111–2117.
25. Johnson, E.F., and S. Kornfeld. 1992. The cytoplasmic tail of the mannose-6-phosphate/insulin-like growth factor-II receptor has two signals for lysosomal enzyme sorting in the Golgi. *J. Cell Biol.* 119:249–257.
26. Johnson, R.G. 1988. Accumulation of biological amines into chromaffin granules: a model for hormone and neurotransmitter transport. *Physiol. Rev.* 68:232–307.
27. Johnston, P.A., P.L. Cameron, H. Stukenbrok, R. Jahn, P. De Camilli, and T.C. Sudhof. 1989. Synaptophysin is targeted to similar microvesicles in CHO and PC12 cells. *EMBO (Eur. Mol. Biol. Organ.) J.* 8:2863–2872.
28. Kelly, R.B. 1991. Secretory granule and synaptic vesicle formation. *Curr. Opin. Cell Biol.* 3:654–660.
29. Kelly, R.B. 1993. Storage and release of neurotransmitters. *Cell.* 72:43–53.
30. Kish, P.E., C. Fischer-Bovenkerk, and T. Ueda. 1989. Active transport of γ-aminobutyric acid and glycine into synaptic vesicles. *Proc. Natl. Acad. Sci. USA.* 86:3877–3881.
31. Koedam, J.A., E.M. Cramer, E. Briend, B. Farie, and D.D. Wagner. 1992. P-selectin, a granule membrane protein of platelets and endothelial cells, follows the regulated secretory pathway in AtT20 cells. *J. Cell Biol.* 116: 617–625.
32. Kuliawat, R., and P. Arvan. 1992. Protein targeting via the "constitutive-like" secretory pathway in isolated pancreatic islets: passive sorting in the immature granule component. *J. Cell Biol.* 118:521–529.
33. Kuliawat, R., and P. Arvan. 1994. Distinct molecular mechanisms for protein sorting within immature secretory granules of pancreatic β-cells. *J. Cell Biol.* 126:77–86.
34. Liu, Y., D. Peter, A. Roghani, S. Schuldiner, G.G. Prive, D. Eisenberg, N. Brecha, and R.H. Edwards. 1992. A cDNA that suppresses MPP+ toxicity encodes a vesicular amine transporter. *Cell.* 70:539–551.
35. Liu, Y., A. Roghani, and R.H. Edwards. 1992. Gene transfer of a reserpine-sensitive mechanism of resistance to MPP+. *Proc. Natl. Acad. Sci. USA.* 89:9074–9078.
36. Liu, Y., E.S. Schweitzer, M.J. Nirenberg, V.M. Pickel, C.J. Evans, and R.H. Edwards. 1994. Preferential localization of a vesicular monoamine transporter to dense core vesicles in PC12 cells. *J. Cell Biol.* 127:1419–1433.
37. Martin, T.F.J. 1994. The molecular machinery for fast and slow neurosecretion. *Curr. Opin. Neurobiol.* 4:626–632.
38. Maycox, P.R., T. Deckwerth, J.W. Hell, and R. Jahn. 1988. Glutamate uptake by brain synaptic vesicles. Energy dependence of transport and functional reconstitution in proteoliposomes. *J. Biol. Chem.* 263:15423–15428.
39. Melega, W.P., and B.D. Howard. 1981. Choline and acetylcholine metabolism in PC12 secretory cells. *Biochemistry.* 20:4477–4483.
40. Melega, W.P., and B.D. Howard. 1984. Biochemical evidence that vesicles are the source of the acetylcholine released from stimulated PC12 cells. *Proc. Natl. Acad. Sci. USA.* 81:6535–6538.
41. Nirenberg, M.J., Y. Liu, D. Peter, R.H. Edwards, and V.M. Pickel. 1995. The vesicular monoamine transporter-2 is present in small synaptic vesicles and preferentially localizes to large dense core vesicles in rat solitary tract nuclei. *Proc. Natl. Acad. Sci. USA.* 92:8773–8777.
42. Nirenberg, M.J., J. Chan, Y. Liu, R.H. Edwards, and V.M. Pickel. 1996. Ultrastructural localization of the vesicular monoamine transporter-2 in midbrain dopaminergic neurons: potential sites for somatodendritic storage and release of dopamine. *J. Neurosci.* 16:4135–4145.
43. Ohno, H., J. Stewart, M.C. Fournier, H. Bosshart, I. Rhee, S. Miyatake, T. Saito, A. Gallusser, T. Kirchhausen, and J.S. Bonifacino. 1995. Interaction of tyrosine-based sorting signals with clathrin-associated proteins. *Science.* 269:1872–1875.
44. Orci, L., M. Ravazzola, M. Amherdt, D. Louvard, and A. Perrelet. 1985. Clathrin-immunoreactive sites in the Golgi apparatus are concentrated at the trans pole in polypeptide hormone-secreting cells. *Proc. Natl. Acad. Sci. USA.* 82:5385–5389.
45. Parsons, S.M., C. Prior, and I.G. Marshall. 1993. Acetylcholine transport, storage and release. *Int. Rev. Neurobiol.* 35:279–390.
46. Peter, D., Y. Liu, C. Sternini, R. de Giorgio, N. Brecha, and R.H. Edwards. 1995. Differential expression of two vesicular monoamine transporters. *J. Neurosci.* 15:6179–6188.
47. Regnier-Vigouroux, A., S.A. Tooze, and W.B. Huttner. 1991. Newly synthesized synaptophysin is transported to synaptic-like microvesicles via constitutive secretory vesicles and the plasma membrane. *EMBO (Eur. Mol. Biol. Organ.) J.* 10:3589–3601.
48. Roghani, A., J. Feldman, S.A. Kohan, A. Shirzadi, C.B. Gundersen, N. Brecha, and R.H. Edwards. 1994. Molecular cloning of a putative vesicular transporter for acetylcholine. *Proc. Natl. Acad. Sci. USA.* 91:10620–10624.
49. Schubert, D., and F.G. Klier. 1977. Storage and release of acetylcholine by a clonal cell line. *Proc. Natl. Acad. Sci. USA.* 74:5184–5188.
50. Schuldiner, S., A. Shirvan, and M. Linial. 1995. Vesicular neurotransmitter transporters: from bacteria to humans. *Physiol. Rev.* 75:369–392.
51. Sollner, T., and J.E. Rothman. 1994. Neurotransmission: harnessing fusion machinery at the synapse. *Trends Neurosci.* 17:344–348.
52. Stinchombe, J.C., and W.B. Huttner. 1994. Purification of secretory granules from PC12 cells. *In* Cell Biology: A Laboratory Handbook. Vol. 1. J.E. Celis, editor. Academic Press, San Diego. 557–566.
53. Südhof, T.C., P. De Camilli, H. Niemann, and R. Jahn. 1993. Membrane fusion machinery: insights from synaptic proteins. *Cell.* 75:1–4.
54. Takei, K., O. Mundigl, L. Daniell, and P. De Camilli. 1996. The synaptic vesicle cycle: a single vesicle budding step involving clathrin and dynamin. *J. Cell Biol.* 133:1237–1250.
55. Thureson-Klein, A. 1983. Exocytosis from large and small dense cored vesicles in noradrenergic nerve terminals. *Neuroscience.* 10:245–259.
56. Tooze, J., and S.A. Tooze. 1986. Clathrin-coated vesicular transport of secretory proteins during the formation of ACTH-containing secretory granules in AtT20 cells. *J. Cell Biol.* 103:839–850.
57. Tooze, S.A., E. Chanat, J. Tooze, and W.B. Huttner. 1993. Secretory granule formation. *In* Mechanisms of Intracellular Trafficking and Processing of Proproteins. CRC Press, Boca Raton, FL. 157–177.
58. Varoqui, H., and J.D. Erickson. 1996. Active transport of acetylcholine by the human vesicular acetylcholine transporter. *J. Biol. Chem.* 271:27229–27232.
59. Walter, P., and A.E. Johnson. 1994. Signal sequence recognition and protein targeting to the endoplasmic reticulum membrane. *Annu. Rev. Cell Biol.* 10:87–119.
60. Weihe, E., M.K. Schafer, J.D. Erickson, and L.E. Eiden. 1994. Localization of vesicular monoamine transporter isoforms (VMAT1 and VMAT2) to endocrine cells and neurons in rat. *J. Mol. Neurosci.* 5:149–164.
61. Weihe, E., J.-H. Tao-Cheng, M.K.-H. Schafer, J.D. Erickson, and L.E. Eiden. 1996. Visualization of the vesicular acetylcholine transporter in cholinergic nerve terminals and its targeting to a specific population of small synaptic vesicles. *Proc. Natl. Acad. Sci. USA.* 93:3547–3552.